



A Passive Magnetic Bearing Flywheel

Mark Siebert, Ben Ebihara, and Ralph Jansen
Ohio Aerospace Institute, Brook Park, Ohio

Robert L. Fusaro and Wilfredo Morales
Glenn Research Center, Cleveland, Ohio

Albert Kascak
U.S. Army Research Laboratory, Glenn Research Center, Cleveland, Ohio

Andrew Kenny
Texas A&M University, College Station, Texas

The NASA STI Program Office . . . in Profile

Since its founding, NASA has been dedicated to the advancement of aeronautics and space science. The NASA Scientific and Technical Information (STI) Program Office plays a key part in helping NASA maintain this important role.

The NASA STI Program Office is operated by Langley Research Center, the Lead Center for NASA's scientific and technical information. The NASA STI Program Office provides access to the NASA STI Database, the largest collection of aeronautical and space science STI in the world. The Program Office is also NASA's institutional mechanism for disseminating the results of its research and development activities. These results are published by NASA in the NASA STI Report Series, which includes the following report types:

- **TECHNICAL PUBLICATION.** Reports of completed research or a major significant phase of research that present the results of NASA programs and include extensive data or theoretical analysis. Includes compilations of significant scientific and technical data and information deemed to be of continuing reference value. NASA's counterpart of peer-reviewed formal professional papers but has less stringent limitations on manuscript length and extent of graphic presentations.
- **TECHNICAL MEMORANDUM.** Scientific and technical findings that are preliminary or of specialized interest, e.g., quick release reports, working papers, and bibliographies that contain minimal annotation. Does not contain extensive analysis.
- **CONTRACTOR REPORT.** Scientific and technical findings by NASA-sponsored contractors and grantees.

- **CONFERENCE PUBLICATION.** Collected papers from scientific and technical conferences, symposia, seminars, or other meetings sponsored or cosponsored by NASA.
- **SPECIAL PUBLICATION.** Scientific, technical, or historical information from NASA programs, projects, and missions, often concerned with subjects having substantial public interest.
- **TECHNICAL TRANSLATION.** English-language translations of foreign scientific and technical material pertinent to NASA's mission.

Specialized services that complement the STI Program Office's diverse offerings include creating custom thesauri, building customized data bases, organizing and publishing research results . . . even providing videos.

For more information about the NASA STI Program Office, see the following:

- Access the NASA STI Program Home Page at <http://www.sti.nasa.gov>
- E-mail your question via the Internet to help@sti.nasa.gov
- Fax your question to the NASA Access Help Desk at 301-621-0134
- Telephone the NASA Access Help Desk at 301-621-0390
- Write to:
NASA Access Help Desk
NASA Center for Aerospace Information
7121 Standard Drive
Hanover, MD 21076



A Passive Magnetic Bearing Flywheel

Mark Siebert, Ben Ebihara, and Ralph Jansen
Ohio Aerospace Institute, Brook Park, Ohio

Robert L. Fusaro and Wilfredo Morales
Glenn Research Center, Cleveland, Ohio

Albert Kascak
U.S. Army Research Laboratory, Glenn Research Center, Cleveland, Ohio

Andrew Kenny
Texas A&M University, College Station, Texas

Prepared for the
36th Intersociety Energy Conversion Engineering Conference
cosponsored by the ASME, IEEE, AIChE, ANS, SAE, and AIAA
Savannah, Georgia, July 29–August 2, 2001

National Aeronautics and
Space Administration

Glenn Research Center

Available from

NASA Center for Aerospace Information
7121 Standard Drive
Hanover, MD 21076

National Technical Information Service
5285 Port Royal Road
Springfield, VA 22100

Available electronically at <http://gltrs.grc.nasa.gov/GLTRS>

A PASSIVE MAGNETIC BEARING FLYWHEEL

Mark Siebert, Ben Ebihara, and Ralph Jansen
Ohio Aerospace Institute
Brook Park, Ohio 44142

Robert L. Fusaro and Wilfredo Morales
National Aeronautics and Space Administration
Glenn Research Center
Cleveland, Ohio 44135

Albert Kascak
U.S. Army Research Laboratory
Glenn Research Center
Cleveland, Ohio 44135

Andrew Kenny
Texas A&M University
College Station, Texas 77843

ABSTRACT

A 100 percent passive magnetic bearing flywheel rig employing no active control components was designed, constructed, and tested. The suspension of the rotor was provided by two sets of radial permanent magnetic bearings operating in the repulsive mode. The axial support was provided by jewel bearings on both ends of the rotor. The rig was successfully operated to speeds of 5500 rpm, which is 65 percent above the first critical speed of 3336 rpm. Operation was not continued beyond this point because of the excessive noise generated by the air impeller and because of inadequate containment in case of failure. Radial and axial stiffnesses of the permanent magnetic bearings were experimentally measured and then compared to finite element results. The natural damping of the rotor was measured and a damping coefficient was calculated.

INTRODUCTION

Actively controlled magnetic bearings are used by industry for rotor levitation. Active magnetic bearings have the disadvantage of requiring complicated control hardware, such as digital signal processors, amplifiers, digital-to-analog converters, analog-to-digital converters, and software. Passive magnetic bearings do not require this hardware; thereby they have the potential to increase system efficiency and reliability. Another advantage of passive magnetic bearings is that larger rotor-stator gaps may be possible since the current for active magnetic bearings is proportional to the square of the rotor-stator gap.

The disadvantages of passive magnetic bearing are that they typically have lower stiffness and lower damping than similar size active magnetic bearings. The stiffness and damping are not adjustable “on-the-fly,” therefore active vibration control cannot be used with passive magnetic bearings.

Passive magnetic bearing systems must have sufficient stiffness and damping built in to allow them to perform over their entire operating range. There have been previous studies on passive bearing systems. Passive magnetic levitation of at least one degree of freedom has been achieved using (1) permanent magnets (Fremerey (2000), Ohji et al (1999), and Jansen and DiRusso (1996)); (2) passive electrodynamic effects (Ting and Tichy (1992), Post et al. (1997), and Post and Ryutov (1997)); (3) superconductors (Hull et al. (1994), Mulcahy et al. (1999), and Hull and Turner (2000)); and, (4) diamagnetic materials (Geim et al. (1999)). Flywheels have been built and tested using several of these types of passive magnetic levitation systems. They seem well suited since high positional accuracy of the rotor and high stiffness values are not typically required in flywheels.

A few studies have also been published on the stiffness and damping of passive magnetic bearing systems. (1) Ohji et al. (1999) investigated the radial disturbance attenuation characteristics of horizontal- and vertical-shaft machines supported radially by permanent magnetic bearings. (2) Fremerey (2000) used

permanent magnetic bearings with eddy-current damping to levitate a 500 Whr energy storage flywheel for an uninterrupted power supply. (3) Satoh et al. (1996) used a mechanical damper attached to the stator magnets in a system with four axes that are passively levitated. (4) Jansen and DiRusso (1996) measured the stiffness and damping of a ferrofluid stabilizer, and the stiffness of permanent magnetic bearings. A ferrofluid stabilizer consists of an axially magnetized disk magnet in a cavity containing a ferrofluid.

Jewel bearings are widely used in electrical measuring instruments such as galvanometers, ammeters, and energy measuring meters. A jewel bearing consists of a ball that spins on an axis perpendicular to the contact area. Jewel bearings have been treated analytically and experimentally. Sankar and Tzenov modeled the motion accuracy of a jewel bearing (1994a) and determined its steady-state dynamics using a free ball and its motion due to friction (1994b).

Spinning ball contact of jewel bearings was experimentally studied at the Glenn Research Center in the late 60's and early 70's. A series of papers were written on the spinning ball contact. Townsend, Dietrich, and Zaretsky (1969) included speed effects on ball spinning torque. Allen and Zaretsky (1970) proposed a microasperity model for the elastohydrodynamic lubrication of a spinning ball on a flat surface. Dietrich, Parker, and Zaretsky (1968) studied the effect of ball-race conformity on spinning friction. Townsend and Zaretsky (1970) studied the effects on ball spinning torque of antiwear and extreme-pressure additives in a synthetic paraffinic lubricant. Allen, Townsend, and Zaretsky (1973) proposed a new generalized rheological model for lubrication of a ball spinning in a nonconforming groove.

The objective of this study was to demonstrate the potential of a simple system that uses only passive components that could be used for flywheels on unmanned satellites. The approach was to use passive magnetic bearings for radial bearing support and jewel bearings for axial support.

BACKGROUND

Earnshaw's Theorem (Earnshaw, 1842) states that if inverse-square-law forces govern a group of charged particles, they can never be in stable equilibrium. The theorem is based on the consequence that the inverse-square-law forces follow the Laplace partial differential equation. Since the solution of this equation does not have any local maxima or minima and only saddle-type equilibrium points exist, there can be no equilibrium. The theorem usually applies to charged particles and magnetic dipoles but also can be extended to solid magnets. Thus, this theorem explains why it is impossible to have a completely 3 dimensionally stable passive magnetic bearing using only the forces of static fields of permanent magnets.

There are five known cases where Earnshaw's Theorem does not apply: (1) time-varying fields, (2) active-feedback systems, (3) diamagnetic systems, (4) ferrofluids, and (5) superconductors. Active feedback control is the most commonly used method to circumvent Earnshaw's Theorem.

The method used by Jansen and DiRusso (1996) was to use a ferrofluid stabilizer. A ferrofluid is a fluid that contains chemically suspended iron-oxide-magnetic particles. The addition of these particles causes the fluid to have magnetic properties. A ferrofluid stabilizer is based upon the interaction between a permanent magnet and a magnetic fluid. A magnet immersed in a ferrofluid will seek an equilibrium position within the magnetic fluid. If the magnet is displaced from its equilibrium position, a restoring force will result. This type of system is stable in all axes, however the load capacity is minimal. To increase the load capacity, a ferrofluid stabilizer was constructed using a restricted cavity for the magnetic fluid. The magnet geometry was optimized in order to increase the restoring force in one axis relative to the other two translational axes.

To stabilize the passive radial magnetic bearing that was built by Jansen and DiRusso (1996), two permanent magnetic disks were mounted on a rotor and two annular magnetic rings were mounted on a stator. The disks were located concentrically within the rings. The outer face of the disk and the inner face of the ring have the same magnetic polarity, which results in a repulsive magnetic force and suspends the rotor. These disks were coupled with a ferrofluid stabilizer on each end of the shaft. This arrangement resulted in a very stable passive magnetic bearing (Figure 1). However, because of the high viscosity of the ferrofluid, there was considerable drag on rotation. Therefore, the bearing could not be used for high-speed applications. However, the bearing does show promise for use with small oscillations and for use as a vibration isolation device.

Jansen and Fusaro initiated the second design. The same type of radial support was used, but a jewel bearing provided the axial support. A photo of this bearing is shown in Figure 2. The bearing was an improvement over the first design, but there was still considerable torque loss on rotation.

For this concept to work a more precise way of aligning the radial magnets would have to be developed. A redesign program was initiated which resulted in the design described in this paper, which is a redesign of bearing in Figure 2.

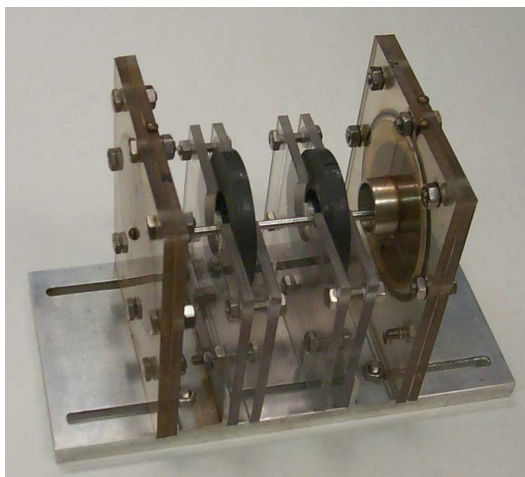


Figure 1. Passive magnetic bearing using ferrofluid stabilizers for the axial stabilization.

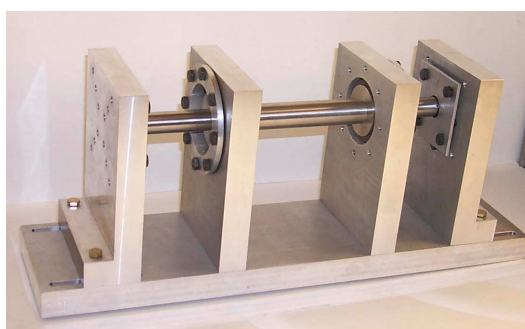


Figure 2. Passive magnetic suspension using jewel bearings for axial stabilization.

DESCRIPTION OF REDESIGNED RIG

The redesigned rig, shown in Figure 3, is an improvement over the previous two rigs in that it incorporates a precise method of aligning the position of the radial magnetic bearings to minimize the axial force. In the two previous designs, the magnetic bearing stators were held by slide fits on the base and alignment was performed by moving the magnetic bearing stators by hand (Figures 1 and 2). In the redesign, load cells were positioned behind each jewel bearing to measure the axial load whereas in the previous two designs no load cells were incorporated. To accomplish this precise alignment, the entire rotor axis of the support base is internally threaded. This allowed the externally threaded stator magnets to be moved along the axis of the rotor during assembly and during fine adjustment of the axial force. Since the threads have little backlash, and the support base and the rotor are stiff, precise alignment is possible.

In the ferrofluidic-stabilized rig shown in Figure 1, each radial magnetic bearing was formed by a single magnet on the stator and a single magnet on the rotor. In the first jewel bearing rig (Figure 2), each magnetic bearing is formed by a stack of two magnets on the stator and two on the rotor. There was a problem aligning the magnetic forces of the rig in Figure 2 so the rotor was never properly positioned. In the redesigned rig, each magnetic bearing is formed by a stack of four magnets on the stator and four on the rotor.

The redesigned rig has a higher radial bearing stiffness than either two previous designs, because of the different radial magnetic bearing design and the use of magnets with a higher energy product. The redesigned rig also has a means of turning the rotor (an air impeller), whereas the previous two did not.

A schematic of the passive magnetic bearing rig is shown in Figure 4. The support base is made of a single piece of aluminum alloy. The rest of the rig consists of two passive magnetic bearings, a wheel, jewel bearings on both ends of the rotor, and an air impeller. The two sets of permanent magnetic bearings operating in the repulsion mode provide levitation in the radial direction. The axial movement of the rotor is constrained by two jewel bearings. Jewel bearings were placed on both ends of the rotor to allow for force reversal.

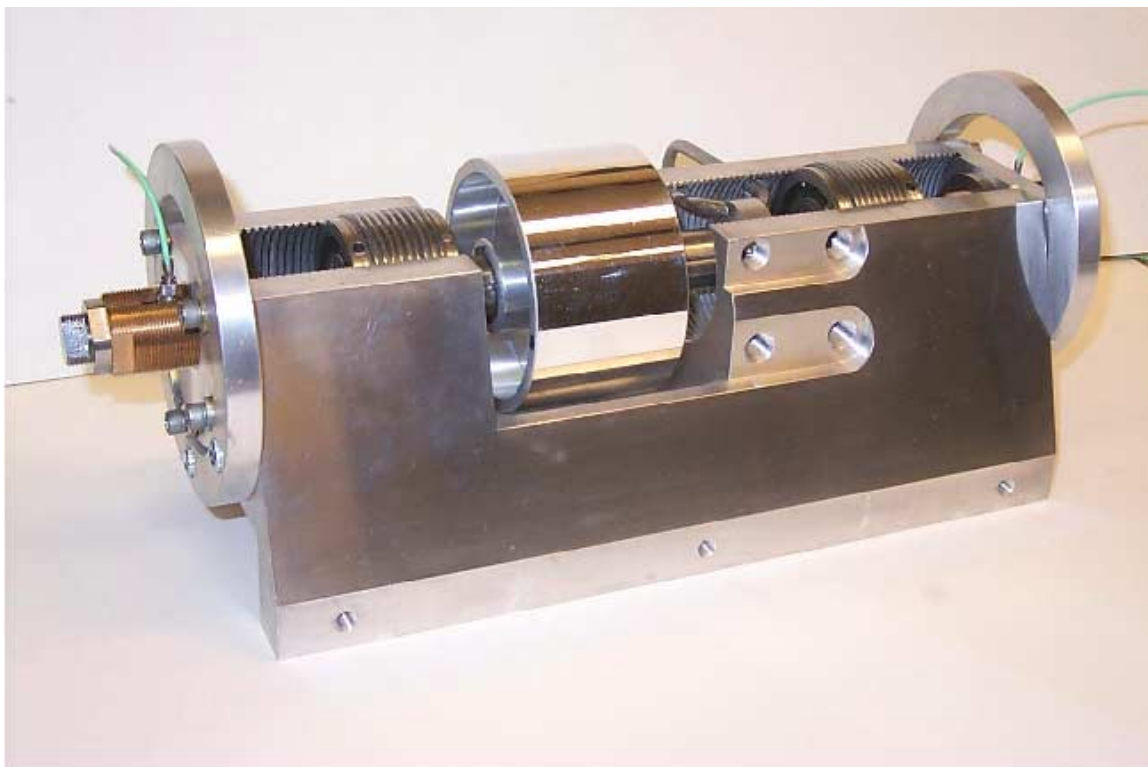


Figure 3. Photographic image of the redesigned jewel bearing rig showing improvements over previous designs.

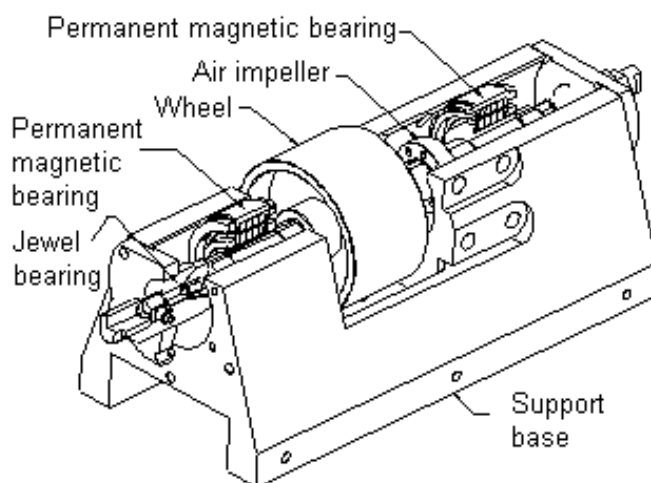


Figure 4. Schematic view of passive magnetic bearing rig. The permanent magnetic bearings and jewel bearing assembly at the near end were sectioned for clarity.

The rotor shaft was made of nonmagnetic stainless steel. The wheel, permanent magnetic bearings and an air impeller were slip fit over the rotor shaft and restrained axially by retaining rings. Each end of the rotor has a ball retainer to hold the 3.175 mm (0.125 inch) diameter ball used in the jewel bearing. The ball retainer is held to the rotor by threads on the rotor bore. The arrangement of components on the rotor is shown in Figure 5.

Figure 6 depicts the permanent magnet bearing assembly. The magnets were axially magnetized, meaning the poles are on the flat sides the magnets. A separate magnet stack was attached to the rotor and to the stator. Four magnet rings comprise each magnet stack. The poles of the magnets were oriented so that the stationary magnets and the rotating magnets repel each other when the non-rotating and the rotating sleeves are axially aligned.

Neodymium-iron-boron (NdFeB) magnets were used, having a nominal BH product of 35 MGOe (Gauss-Oersted $\times 10^6$). The dimensions of the rotating and stationary magnets are as follows. The OD of the rotating magnet is 45.7 mm (1.800 in) and the ID is 31.8 mm (1.250 in). The stationary magnet OD is 61.0 mm (2.400 in) and the ID is 48.3 mm (1.900 in). The thickness of magnet rings used in both stacks is 5.08 mm (0.200 inch). Therefore, the total axial thickness of the magnets in each stack is nominally 20.3 mm (0.800 inch).

Both the non-rotating and the rotating sleeves were made of nonmagnetic stainless steel. The stacks of magnets and the nonconductive spacers were connected together with epoxy in their mounting sleeve. The magnets were stacked with like poles adjacent to each other (NS-SN-NS-SN) and permanently locked in place with epoxy. During the assembly process each magnet was coated with epoxy and put in the sleeve along with the nonconductive spacers and the sleeve end ring. An arbor press was used to provide the force to hold the magnets in the sleeve while press pins could be installed in the sleeve end ring. Once the sleeves were assembled, a thin coat of epoxy was also applied to the free surface of the magnets to prevent the magnets from oxidizing.

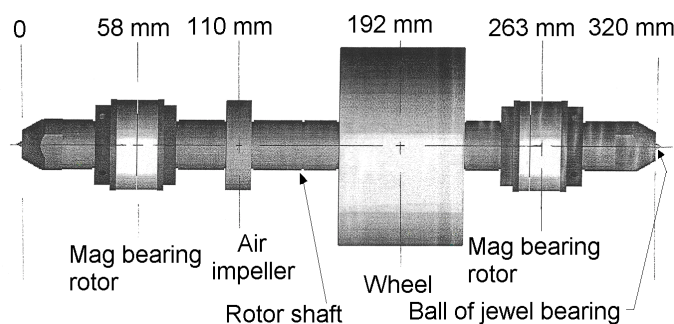


Figure 5. Schematic of rotor that shows the location of components. The total mass of the rotor is 2.26 kg. The diameter of the wheel is 102 mm.

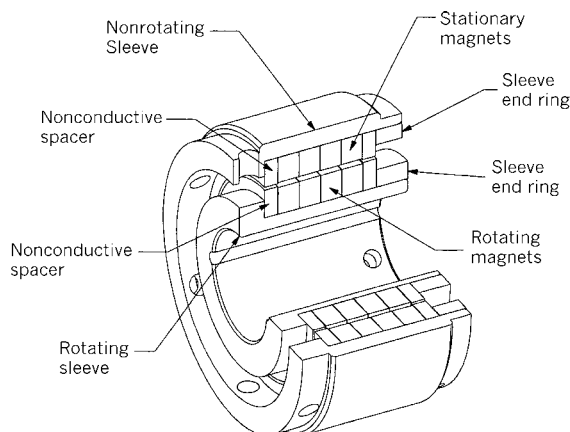


Figure 6. Sectioned view of permanent magnetic bearing assembly. There are two of these assemblies attached to the rotor.

The OD of the nonrotating magnet sleeve was threaded. These threads fit the threading along the rotor axis of the support base, allowing the stator magnets to be moved axially. The stator magnet sleeve was rotated by inserting a Ø4.75mm rod into a hole on the end of this sleeve. The rod was turned until the stationary sleeve was positioned over the rotating sleeve. The stator magnets were adjusted to minimize the axial force before operation.

The rotating and stationary magnets had a nominal 1.27 mm (0.05 inch) radial gap. The nonconductive spacers on the rotor and the stator were axially aligned and have a 0.76 mm (0.03 inch) nominal gap. This smaller clearance was to prevent the rotor and stator magnets from contacting during installation and operation.

A schematic of the jewel bearing assembly is shown in Figure 7. The jewel bearing on each end of the rotor consisted of a removable 3.175 mm (0.125 inch) diameter Si_3N_4 ball held in the ball retainer in the center of the rotor shaft. About 0.50 mm (0.02 inch) of the ball extends beyond the surface of the ball retainer. The ball spins against the stationary 440C stainless steel disk of the jewel bearing. The surface of the disk was perpendicular to the axis of the rotor. A piezoelectric load cell measures the load of the jewel bearing contact.

An air impeller drives the shaft. The air impeller is a disk with blind holes drilled on both sides. One air stream is directed to either side of the disk to minimize the radial force on the rotor. The blind holes catch the air, and rotate the rotor.

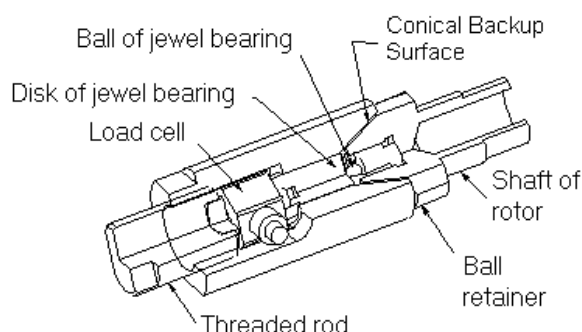


Figure 7. Jewel bearing assembly applied to each end of the rotor. The ball of the jewel bearing rotates against the stationary disk of the jewel bearing during operation.

RESULTS AND DISCUSSION

Spin Testing

The rotor was spun by using an air impeller. A 120-psig-air line was connected to a pressure regulator leading to the air impeller. Adjusting the flow rate of the compressed air against the impeller could control the rotational speed of the bearing. A stroboscope was used to monitor the rotational speed.

Testing consisted of slowly increasing the speed. The speed was gradually increased to 5500 rpm and the bearing ran very smoothly over the entire speed range. It was stopped at this point only because of the loud noise generated by the compressed air and also, for safety (there was not any shielding around the bearing). Other than these two reasons, there was nothing observed that would have prevented the bearing from being run at much higher speeds.

The rotor passed through a critical speed at 3336 rpm, but no resonant vibrations were observed. This critical speed was found by impact testing of the rotor and is discussed later in the paper. The tests were repeated a second time and still no vibrations were observed.

Radial and Axial Stiffnesses of Bearings

The procedure for experimentally measuring the radial magnetic bearing stiffness was to direct the axial force to one jewel bearing by adjusting the magnetic bearing stators. The disk part of the jewel bearing at the other end of the rotor was removed so that the rotor was free to rotate about the contacting jewel bearing. Two dial indicators were contacted against the shaft to measure the radial deflection. One dial indicator was positioned 40 mm from the free end of the rotor. The other dial indicator was positioned 25mm from the contacting jewel bearing. The rotor was deflected by adding weights to the shaft near the free end. The deflections of both dial indicators were recorded as a function of applied load. The moments about the existing

jewel bearing were computed for each load applied and these were used to calculate the stiffness of the passive magnetic bearings. Analysis of the two dial indicator readings showed that the ball of the jewel bearing was not laterally displaced when the weights were loaded on the rotor. The force versus deflection characteristics of one passive magnetic bearing was calculated from the load versus deflection curve.

To predict the stiffness of the permanent magnetic bearing by the finite element method, a finite element model was made for the permanent magnet rings. The model had 77760 linear brick elements as shown in Figure 8. A magnetostatic solver was used to compute the distribution of the magnetic field. The Maxwell stress tensor was integrated over the surface of the four inner ring magnets to calculate the force on them.

Figure 9 shows the displacement as a function of radial load for the finite element and experimental data. In order to compare the experimental and the finite element results, linear regression curve fits were performed. The slope of the experimental curve is 1.78×10^5 N/m (1.02×10^3 lb_f/in). The slope of the finite element curve is 1.87×10^5 N/m (1.07×10^3 lb_f/in). The radial stiffness found by the experimental method is about 5.2 percent less than the finite element prediction. This is considered very good agreement.

The radial stiffness per unit length of the magnet stack of each bearing was calculated by dividing the experimental radial stiffness, 1.78×10^5 N/m (1.02×10^3 lb_f/in) by the length of each magnet stack, 20.3mm (0.800 in). This value is 8.76×10^6 (N/m)/m (1.27×10^3 (lb_f/in)/in).

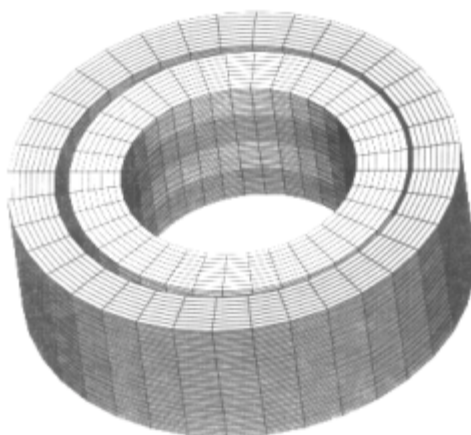


Figure 8. Finite element model of ring magnets in magnetic bearing.

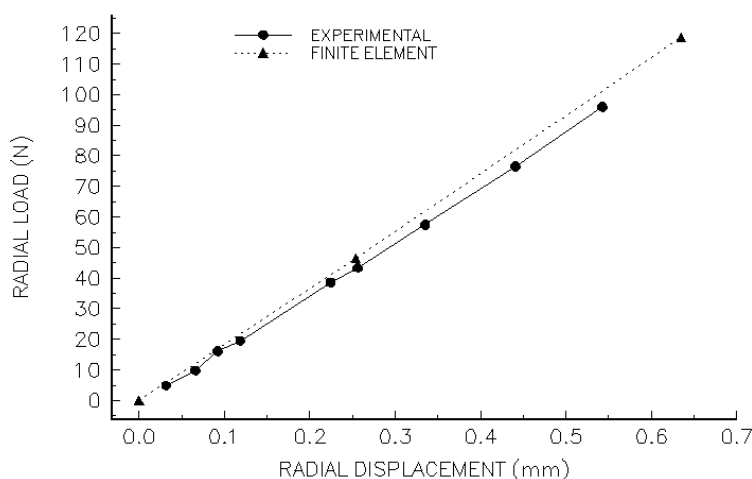


Figure 9. Radial displacement as a function of radial load for one permanent magnetic bearing as determined by experimental testing and finite element analysis.

To measure the axial stiffness, one non-rotating magnetic bearing sleeve was rotated by means of the threading in the support base. This caused the magnet stacks to become axially displaced relative to each other. This axial displacement was measured with a dial indicator. The axial load due to this displacement was measured with the load cell positioned behind the disk of the jewel bearing. This procedure was repeated for a number of different displacements and the data plotted in Figure 10. The figure shows that the axial load is a linear function of displacement for this permanent magnetic bearing. A linear regression fit of the curve gave a value of 3.52×10^5 N/m (2.01×10^3 lb_f/in) for the axial stiffness of one bearing.

Application of Earnshaw's theorem implies that the axial stiffness should be exactly twice the radial stiffness. Comparing the experimental axial stiffness of Figure 10 [3.52×10^5 N/m (2.01×10^3 lb_f/in)] to twice the experimental radial stiffness of Figure 9 [1.78×10^5 N/m (1.02×10^3 lb_f/in)] showed that the 2 to 1 ratio predicted by Earnshaw's theorem is within 1.1 percent. This is considered very good agreement.

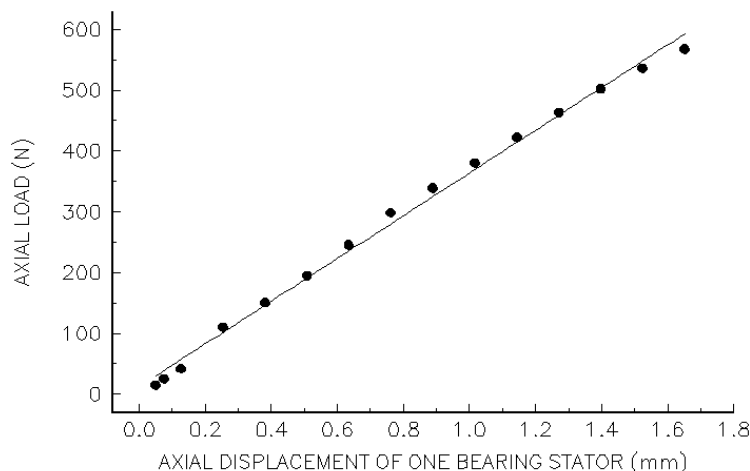


Figure 10. Axial displacement as a function of axial load for one magnetic-bearing stator of the permanent magnetic bearing.

Damping

The procedure for measuring the free vibration history of the rotor was as follows. An axial force on one of the jewel bearings was produced by misalignment of the stationary magnets and then rotating magnets of the magnetic bearing. The disk of the jewel bearing at the unloaded end of the rotor was removed so that the rotor was free to move about this end. An accelerometer was attached to the rotor 25 mm from free end. To excite the rotor, the wheel was struck radially with an impact hammer. Figure 11 gives the radial free vibration history of the rotor as a function of time. The rotor was “pinned” against only one jewel bearing since during operation only one jewel bearing is in contact. These conditions resulted in only one mode, not a bounce and a tilt mode as would occur with “free-free” boundary conditions.

A radial damping coefficient was calculated from the logarithmic decrement and from the half-power bandwidth methods. The natural logarithm of consecutive amplitude ratios is called the logarithmic decrement, δ , equaling $\ln(x_1/x_2)$, where x_1 and x_2 are consecutive peak amplitudes. The log decrement is a measure of the damping factor ξ and it gives a convenient method to measure the damping in a system. The damping coefficient is related to the log decrement, by $\delta = 2\pi\xi/(1-\xi^2)^{0.5}$. Taking the log decrement of the first five peaks in the time domain gives $\xi = 0.0649$, or about 6.5 percent damping. The radial frequency response of the rotor is shown in Figure 12. The first fundamental occurred at 55.6 Hz (3336 rpm). From the frequency response data, the damping coefficient of the first fundamental was calculated by the half-power bandwidth method. The damping coefficient of the first fundamental was found to be 0.069, close to the damping coefficient as found by the logarithmic decrement method. Since no vibrations were observed on running the bearing through the critical speed, 6.5 percent damping is adequate to control the rotor.

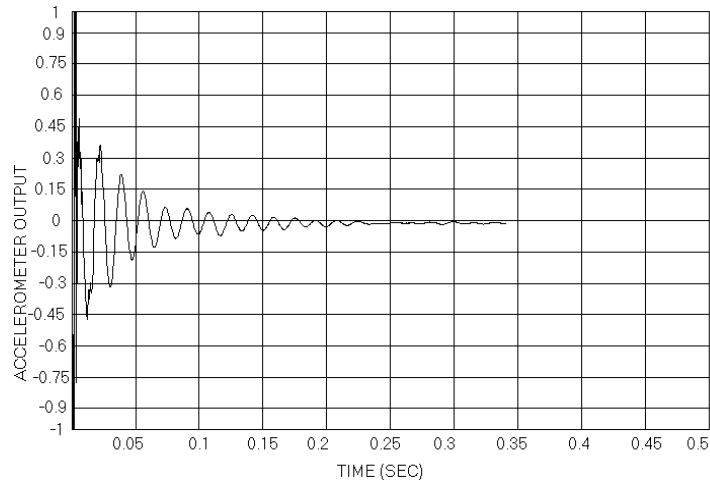


Figure 11. Radial free vibration history of the rotor from an impact test. The vertical axis is the output of the accelerometer attached to the free end of the rotor.

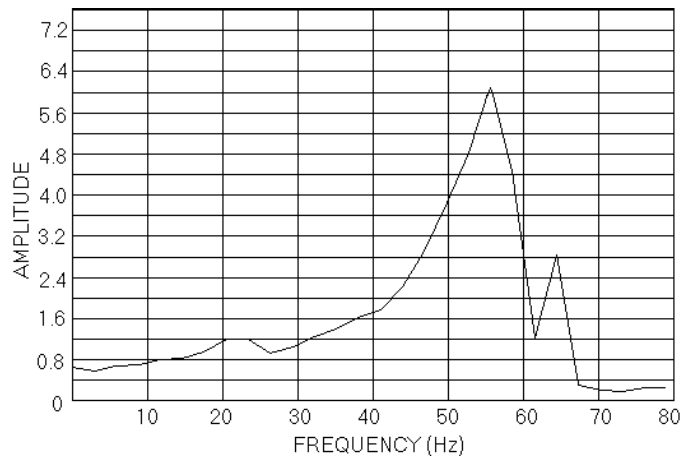


Figure 12. Frequency response of the rotor that occurred from impact test.

SUMMARY OF RESULTS

A completely passive magnetic bearing rig was designed, constructed, and tested. Support of the rotor was accomplished in the radial direction by two sets of permanent magnetic bearings and in the axial direction by two sets of jewel bearings. The following results were obtained.

1. The rig was successfully operated to a speed of 5500 rpm, which was 65 percent above the first critical speed.
2. The radial stiffness of one magnetic bearing was measured to be 1.78×10^5 N/m (1.02×10^3 lb_f/in) which was within 5 percent of a finite element prediction. The measured stiffness was adequate for the currently designed rotor.
3. The fact that experimental and finite element methods predictions agree demonstrate that finite element methods can be used to accurately design the size and number of the magnets for the radial support of the bearings.

4. The radial damping for the first fundamental was measured to be 6.5 percent of critical damping. This was adequate damping to pass through the first critical speed.
5. The axial stiffness was measured and was shown to be within 1 percent of twice the measured radial stiffness. This is consistent with Earnshaw's theorem.

REFERENCES

- Allen, C.W., Zaretsky, E.V., 1970, "Microasperity Model for Elastohydrodynamic Lubrication of a Spinning Ball on a Flat Surface," NASA TN D-6009.
- Allen, C.W., Townsend, D.P., and Zaretsky, E.V., 1973, "New Generalized Rheological Model for Lubrication of a Ball Spinning in a Nonconforming Groove," NASA TN D-7280.
- Dietrich, M.W., Parker, R.J., Zaretsky, E.V., 1968, "Effect of Ball-Race Conformity on Spinning Friction," NASA TN D-4669.
- Earnshaw, S., 1842, "On the Nature of the Molecular Forces which Regulate the Constitution of the Luminiferous Ether," *Trans. Of the Cambridge Philosophical Society*, Vol. 7, Part I, pp. 97-112.
- Fremerey, J.K., 2000, "A 500-Wh Power Flywheel on Permanent Magnet Bearings," Fifth International Symposium on Magnetic Suspension Technology, pp. 287-295.
- Geim, A.K., Simon, M.D., Boamfa, M.I., and Heflinger, L.O., 1999, "Magnetic Levitation at Your Fingertips," *Nature*, Vol. 400, pp. 232-324.
- Hull, J.R., Mulcahy, T.M., Uherka, K.L., Erck, R.A., and Abboud, R.G., "Flywheel Energy Storage Using Superconducting Magnetic Bearings," *Appl. Supercond.*, Vol. 2, pp. 449-455, July/Aug. 1994.
- Hull, J.R., and Turner, L.R., 2000, "Magnetomechanics of Internal-Dipole, Halbach-Array Motor/Generators," *IEEE Transactions on Magnetics*, Vol. 36, No. 4, pp. 2004-2011.
- Jansen, R., DiRusso, E., 1996, "Passive Magnetic Bearing with Ferrofluid Stabilization," NASA TM-107154.
- Mulcahy, T.M., Hull, J.R., Uherka, K.L., Niemann, R.C., Abboud, R.G., Juna, J., and Lockwood, T.A., 1999, "Flywheel Energy Storage Advances Using HTS Bearings," *IEEE Trans. Appl. Supercond.*, Vol. 9, pp. 297-300.
- Ohji, T., Mukhopadhyay, S.C., Iwahara, and Yamada, S., 1999, "Permanent Magnet Bearings for Horizontal- and Vertical-Shaft Machines: A Comparative Study," *Journal of Applied Physics*, Vol. 31, 8, pp. 4648-4650.
- Post, R.F., Ryutov, D.D., Smith, J.R., and Tung, L.S., 1997, "Research on Ambient-Temperature Passive Magnetic Bearings at the Lawrence Livermore National Laboratory," LLNL Pub. #231803.
- Post, R.F., Ryutov, D.D., 1997, "Ambient-Temperature Passive Magnetic Bearings: Theory and Design Equations," LLNL Pub. #232382.
- Sankar, T.S., and Tzenov, P.I., 1994a, "Friction and Motion Accuracy in Jewel Bearing," *Tribology Transactions*, Vol. 37, 2, pp. 269-276.
- Sankar, T.S., and Tzenov, P.I., 1994b, "The Steady-State Dynamics of Jewel Bearing with a Free Ball," *Tribology Transactions*, Vol. 37, 2, pp. 403-409.
- Satoh, I., Shirao, Y., and Kanemitsu, Y., 1996, "Dynamics and Vibration of a Single Axis Active Magnetic Bearing System for Small-Sized Rotating Machinery," Fifth International Symposium on Magnetic Bearings, pp. 497-502.
- Ting, L., Tichy, J., 1992, "Stiffness and Damping of an Eddy Current Magnetic Bearing," *Journal of Tribology*, Vol. 114, July, pp. 600-604.
- Townsend, D.T., and Zaretsky, E.V., 1970, "Effects of Antiwear and Extreme-Pressure Additives in a Synthetic Paraffinic Lubricant on Ball Spinning Torque," NASA TN D-5820.
- Townsend, D.P., Dietrich, M.W., Zaretsky, E.V., 1969, "Speed Effects on Ball Spinning Torque," NASA TN D-5527.

REPORT DOCUMENTATION PAGE			Form Approved OMB No. 0704-0188	
Public reporting burden for this collection of information is estimated to average 1 hour per response, including the time for reviewing instructions, searching existing data sources, gathering and maintaining the data needed, and completing and reviewing the collection of information. Send comments regarding this burden estimate or any other aspect of this collection of information, including suggestions for reducing this burden, to Washington Headquarters Services, Directorate for Information Operations and Reports, 1215 Jefferson Davis Highway, Suite 1204, Arlington, VA 22202-4302, and to the Office of Management and Budget, Paperwork Reduction Project (0704-0188), Washington, DC 20503.				
1. AGENCY USE ONLY (Leave blank)		2. REPORT DATE February 2002		3. REPORT TYPE AND DATES COVERED Technical Memorandum
4. TITLE AND SUBTITLE A Passive Magnetic Bearing Flywheel			5. FUNDING NUMBERS WU-274-00-00-00	
6. AUTHOR(S) Mark Siebert, Ben Ebihara, Ralph Jansen, Robert L. Fusaro, Wilfredo Morales, Albert Kascak, and Andrew Kenny				
7. PERFORMING ORGANIZATION NAME(S) AND ADDRESS(ES) National Aeronautics and Space Administration John H. Glenn Research Center at Lewis Field Cleveland, Ohio 44135-3191			8. PERFORMING ORGANIZATION REPORT NUMBER E-13017	
9. SPONSORING/MONITORING AGENCY NAME(S) AND ADDRESS(ES) National Aeronautics and Space Administration Washington, DC 20546-0001			10. SPONSORING/MONITORING AGENCY REPORT NUMBER NASA TM-2002-211159 IECEC2001-AT-89	
11. SUPPLEMENTARY NOTES Prepared for the 36th Intersociety Energy Conversion Engineering Conference cosponsored by the ASME, IEEE, AIChE, ANS, SAE, and AIAA, Savannah, Georgia, July 29-August 2, 2001. Mark Siebert, Ben Ebihara, and Ralph Jansen, Ohio Aerospace Institute, 22800 Cedar Point Road, Brook Park, Ohio 44142; Robert L. Fusaro and Wilfredo Morales, NASA Glenn Research Center; Albert Kascak, U.S. Army Research Laboratory, NASA Glenn Research Center; Andrew Kenny, Texas A&M University, College Station, Texas 77843. Responsible person, Robert L. Fusaro, organization code 5950, 216-433-6080.				
12a. DISTRIBUTION/AVAILABILITY STATEMENT Unclassified - Unlimited Subject Category: 20 Available electronically at http://gltrs.grc.nasa.gov/GLTRS This publication is available from the NASA Center for AeroSpace Information, 301-621-0390.			12b. DISTRIBUTION CODE	
13. ABSTRACT (Maximum 200 words) A 100 percent passive magnetic bearing flywheel rig employing no active control components was designed, constructed, and tested. The suspension of the rotor was provided by two sets of radial permanent magnetic bearings operating in the repulsive mode. The axial support was provided by jewel bearings on both ends of the rotor. The rig was successfully operated to speeds of 5500 rpm, which is 65 percent above the first critical speed of 3336 rpm. Operation was not continued beyond this point because of the excessive noise generated by the air impeller and because of inadequate containment in case of failure. Radial and axial stiffnesses of the permanent magnetic bearings were experimentally measured and then compared to finite element results. The natural damping of the rotor was measured and a damping coefficient was calculated.				
14. SUBJECT TERMS Space; Mechanisms; Bearings; Flywheel; Energy storage			15. NUMBER OF PAGES 16	
			16. PRICE CODE	
17. SECURITY CLASSIFICATION OF REPORT Unclassified	18. SECURITY CLASSIFICATION OF THIS PAGE Unclassified	19. SECURITY CLASSIFICATION OF ABSTRACT Unclassified	20. LIMITATION OF ABSTRACT	